Kazemi and Ghiasvand *International Journal of Mechanical and Materials Engineering* (2021) 16:8
https://doi.org/10.1186/s40712-021-00131-9

International Journal of Mechanical and Materials Engineering

ORIGINAL PAPER Open Access

Effect of cone angle of cylindrical pin in the SFSW and DFSW on mechanical properties of AA6061-T6 alloy

Mahdi Kazemi[1*] and Amir Ghiasvand[2]

Abstract

In the present study, the effect of cone angle of tool pin on the mechanical properties and microhardness properties of aluminum alloy AA6061-T6 specimens is investigated for three processes of SFSW, symmetric DFSW, and asymmetric DFSW. In each of the mentioned welding processes, tools with 5 different conical angles of 0, 5, 10, 15, and 20° are used. In these three welding processes, the mechanical properties of the final welded joint with conical tools have been enhanced noticeably compared to the tool with simple cylindrical pins (0° angle). Based on the obtained results, it was found that the joints obtained from asymmetric DFSW, symmetric DFSW, and SFSW had the best mechanical properties, respectively. The optimum cone angles for tool pin in SFSW, symmetric DFSW, and asymmetric DFSW processes were equal to 15, 10, and 10°, respectively. In addition, it was concluded that the welded specimen through the asymmetric DFSW with the cone angle of 10° attained the closest mechanical properties to the base (parent) metal. The parameters of YS, UTS, and E% in this sample were 78.3%, 84.8%, and 86.4% of the base sample, respectively.

Keywords: Friction stir welding, Tool geometry, Mechanical properties, Microhardness, Aluminum alloy

Introduction

Friction stir welding (FSW) is a relatively novel technique, through which, high-quality mechanical and metallurgical joints can be created in components without local melting (Mishra et al., 2014). This process is classified as solid-state bonding process that is conducted as a result of exerted pressure and large plastic deformation. The presence of appropriate plastic flow during the FSW process would improve the mechanical properties of the welded specimen and provide a joint with optimal quality. The several affecting factors and parameters on the final quality of the joint would lead to the particular complexities of FSW process despite its simple structure. In general, the influential factors in FSW process are categorized into three general groups of process parameters, tool geometry, and joint geometry (Devaiah et al., 2018; Dialami et al., 2017; Yang et al., 2013). These three groups have several subgroups, which complicate the effectiveness and interaction of FSW factors (Yaduwanshi et al., 2018). Tool and joint geometries are known as the most important factors, which determine the volume and shape of the plastic material flow. Changing the geometrical parameters of the tool would lead to a significant change in the material flow, which affects the final quality of the joint (Zettler et al., 2005). Cone angle of the cylindrical pins can be mentioned as the most important parameter of the tool geometry. According to the conducted studies, it was found that the use of conical tools improves the quality and mechanical properties of the final joint compared to the cylindrical ones. By creating an optimum cone angle in the tool pin, the temperature gradient in the joint components would be changed, and consequently, the volume of plastic flow and pattern of the horizontal and vertical material flows would also be varied. This phenomenon results in an improved final joint quality and elimination of process

* Correspondence: kazemii.m@gmail.com; kazemi@malayeru.ac.ir
[1]Department of Mechanical Engineering, Faculty of Engineering, Malayer University, Malayer, Iran
Full list of author information is available at the end of the article

defects up to a high degree. Changing the cone angle is corresponding to the change in the volume of pumped flow to the bottom of the workpiece. Proper material flow in the workpiece increases the possibility of creating an appropriate and defect-free joint in that area. Other possible ways for reducing the process imperfections and enhancing the weld quality in the bottom of the workpiece include changing the geometry and joining process (Baker et al., 2019; Lohwasser & Chen, 2009; Rai et al., 2011; Zhang et al., 2012). Generally, the joint geometry used in FSW butt welding comprises single-sided friction stir welding (SFSW) and double-sided friction stir welding (DFSW). Commonly, SFSW is used in the welding process of parts with small thicknesses, while in relatively thick parts DFSW is utilized (Baker et al., 2019). Symmetry or asymmetry of the DFSW process is the important factor to be considered in DFSW. If after welding the upper and lower surfaces of the workpiece the advancing side (AS) overlaps the retreating side (RS), the DFSW is considered symmetric; otherwise, it is called asymmetric. Symmetry or asymmetry in the DFSW process affects the mechanical properties of the joint significantly. So far, very little research has been performed considering the effect of tool cone angle on the mechanical properties of SFSW joint. Ramachandran, Murugan, and Kumar et al. (Ramachandran et al., 2015) investigated the effect of cone angle and tool offset on the mechanical and metallographic properties of bonding two non-homogeneous materials of AA5052 aluminum alloy and HSLA steel using SFSW. According to their results, offset towards harder metal and the use of a cylindrical tool had improved the mechanical and metallurgical properties of the joint, considerably. Ugender, Kumar, and Reddy (Ugender et al., 2014) investigated the mechanical properties of the joint from cylindrical and conical tools in SFSW of AA2014 aluminum alloy. Based on their results, it was found that the use of conical tool resulted in a significant increase in the ultimate tensile strength (UTS) and elongation percentage (E%) of the specimens compared to cylindrical tools. Gadakh and Adepu (Gadakh & Adepu, 2013) developed an analytical model to calculate the maximum temperature (T_{max}) of SFSW process with a conical pin tool. The results of the analytical model revealed that increasing the cone angle would decrease T_{max} as well as the generated heat in the process. The mechanical properties of samples obtained from SFSW and DFSW of the A1100 H14 alloy were investigated by Kumar, Varghese, and Sivapragash (Kumar et al., 2012). According to the obtained results, it was found that the mechanical strength of DFSW specimens were better than the SFSW specimens. Additionally, better mechanical properties of asymmetric DFSW specimens than symmetric DFSW process were reported. Hejazi and Mirsalehi (Hejazi & Mirsalehi, 2016) investigated the effect of pin penetration (pin length) on the mechanical and microstructural properties of the joints obtained by SFSW and DFSW processes. Based on the results, by the selection of optimal pin length in DFSW, the UTS increased significantly compared to SFSW. Xu, Wang, Luo, Li, and Fu (Xu et al., 2018) investigated the effect of process parameters and strain rate on the mechanical properties of AA7085-T7452 alloy after DFSW process. They illustrated that the reduction of strain rate in DFSW process increases the yield stress (YS) as well as E% besides the reduction of UTS. Ghiasvand, Kazemi, Mahdipour Jalilian and Ahmadi Rashid (Ghiasvand et al, 2020) investigated the effects of pinshift, tool offset and alloy position on the maximum processtemperature. Based on analysis of variance, pin shift was themost effective variable at maximum temperature. By shiftingthe pin, a decrease in the maximum temperature was observed. Offset of the tool causes the maximum temperature to drop;however, this drop is more severe on the advancing side. Ghiasvand, Kazemi, Mahdipour Jalilian (Ghiasvand et al, 2021) investigated the grain size in different welded areas by using the analytical-numerical method based on the simulation of FSW finite elements of AA6061-T6 alloy. By reviewing the available literature, it is found that the cone angle of the cylindrical tool pin has not been specifically addressed in previous studies, and no research has been conducted on the optimization of this factor. Moreover, the effect of cone angle on symmetric and asymmetric DFSW processes has not been considered yet. Therefore, the present study investigates the effect of cone angle on the mechanical and microhardness properties of the samples obtained from the SFSW, symmetric DFSW, and asymmetric DFSW processes of AA6061-T6 aluminum alloy.

Materials and experimental method

In the present study, the effect of cone angle of conical tools on the mechanical and microhardness properties of joints obtained by SFSW, symmetric DFSW, and asymmetric DFSW processes was investigated. As mentioned, in the symmetric DFSW process, the identical weld zones in upper and lower welding stages overlap each other, while in the asymmetric DFSW the reverse condition occurs. The schematics of the FSW, symmetric DFSW, and asymmetric DFSW processes are shown in Fig. 1.

The SFSW process was carried out in one welding pass, and the symmetric and asymmetric DFSW processes were performed in two welding passes (welding upper and lower surfaces of the workpiece). To apply the second pass in DFSW process, after conducting the first welding pass (upper surface welding), the workpiece was cooled to ambient temperature. After cooling and reversing the workpiece, the second pass of welding

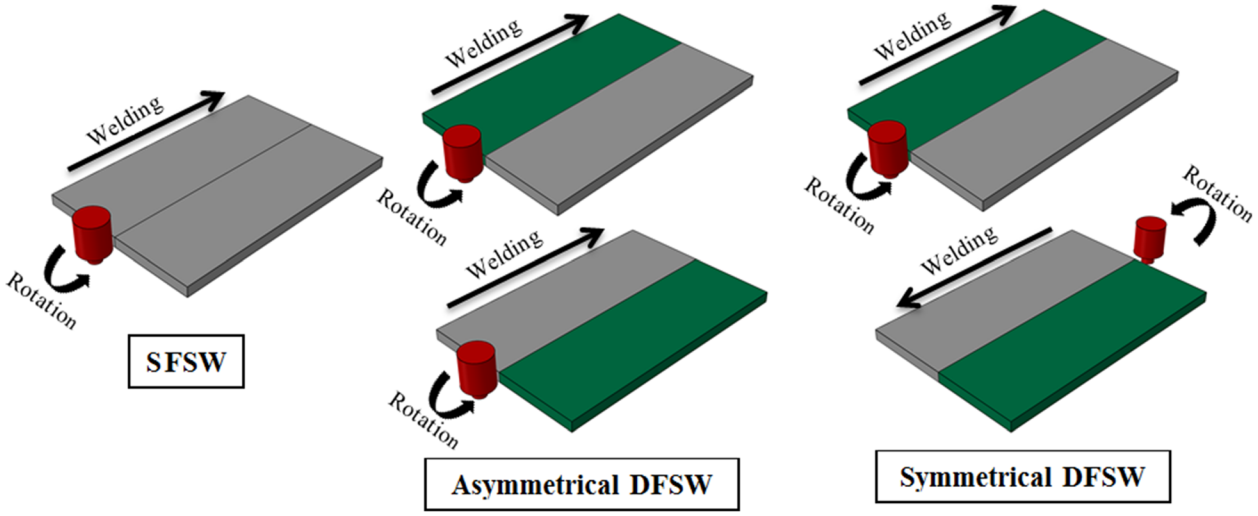

Fig. 1 The schematic of the FSW, symmetric DFSW, and asymmetric DFSW processes

(lower surface welding) was performed. It should be noted that the traverse speed and angular velocity in all three processes were assumed to be 100 mm/min and 1180 rpm, respectively. Moreover, a suitable milling machine and a clamping fixture were used for conducting the welding process. Figure 2 shows an overview of the used milling machine and fixture.

In order to perform three desired welding processes, the specimens with the dimensions of 120×50×5 mm were used. Before welding, all specimens were subjected to a surface polishing so that the possible imperfections in the Nugget Zone were eliminated. All the specimens were made of AA6061-T6 aluminum alloy. The chemical compositions and mechanical properties of the AA6061-T6 alloy are provided in Tables 1 and 2, respectively.

To investigate the effect of cone angle in SFSW and symmetric and asymmetric DFSW processes, 5 tools with 5 different cone angles of 0, 5, 10, 15, and 20° were used.

Fig. 2 The view of used milling machine and fixture

Table 1 The chemical compositions of AA6061-T6 alloy

Chemical composition (%)								
Al	Mg	Si	Cu	Fe	Cr	Mn	Zn	Ti
Balance	0.81	0.61	0.29	0.2	0.13	0.03	0.02	0.01

The diameter of the tool shoulder was considered 20 mm in all cases, and the pin diameter in the tool shoulder was assumed to be 6 mm. Pin lengths in the SFSW and DFSW processes were 4.7mm and 2.7mm, respectively. Furthermore, the tool penetration in workpiece for SFSW and DFSW specimens were corresponding to 0.1 mm and 0.05 mm. Moreover, dwell time was considered 5 s for all studied specimens. A total of 10 tools were fabricated to perform the SFSW and symmetric and asymmetric DFSW processes. The tools were made of H13 hot work steel. To increase the hardness of the tools, the thermal hardening operations were performed in accordance with the standard (Totten, 2006). Figure 3 shows the used tools in the FSW and DFSW processes.

A total of 15 welding processes with different welding types and cone angles were performed. In Table 3, the parameters for 15 experimental models along with the intended name for each model are listed. Additionally, the welded specimens are depicted in Fig. 4.

Tensile tests and microhardness tests were conducted to investigate the mechanical properties of the welded specimens. Tensile test specimens were manufactured in accordance with ASTM-E8 standard (Astm, 1997). The schematics of tensile test specimens are presented in Fig. 5. It should be noted that two specimens were prepared for each tensile test, and the average of the results was reported as the final value. The tensile tests were done by the use of SANTAM-25KN servo hydraulic machine. The tests were performed under displacement control with the speed of 1 mm/min. The tensile testing machine and the prepared tensile test specimens are depicted in Figs. 6 and 7, respectively.

In order to test the hardness and determine the distribution of Vickers microhardness in different welding regions, a cut from the middle section of each welded specimen was prepared. The surfaces were polished and prepared using sander surfaces of 220, 320, 500, 800, and 1200 for microscopic testing. Microhardness testing of samples was performed by Illinois 60044 microhardness tester manufactured by USA Buehler Ltd. The tests were conducted in the University of Malayer during 30 s under 50 gr load at the ambient temperature. To record the microhardness distribution, 15 points in the mid-depth (2.5-mm thick) section and normal to the weld line were considered. Figure 8 shows the samples prepared for microhardness testing, and Fig. 9 displays the used equipment for microhardness testing and penetration effect on one of the specimen.

Table 2 The mechanical properties of AA6061-T6 alloy

Yield stress (MPa)	UTS (MPa)	Elongation (%)
268	311	17

Results and discussions

Tensile test

In accordance with the explanations given in the previous section, a total of 30 specimens were prepared for tensile testing of 15 experimental models. It should be noted that the average of the two tensile tests for each experimental model was reported as the final value. Yield stress (YS), ultimate strength (UTS), elongation (E%), and fracture position were considered as the studied parameters. The results of these parameters for the investigated models are provided in Table 4. The fracture of the welded specimens may mainly occur in four regions. These regions are known as Nugget Zone (NZ), thermo-mechanically affected zone (TMAZ), heat-affected zone (HAZ), and base metal (BM). In FSW processes, depending on the type and condition of the joint, final fracture may occur in the AS or RS.

The diagrams of YS and UTS for SFSW and symmetric and asymmetric DFSW processes are presented in Figs. 10 and 11, respectively.

The tool cone angle and the features of tool pin are influential parameters in the formation of vertical material flow (plastic flow along the thickness of the workpiece) in the FSW process. In the absence of these two factors, the vertical material flow in the FSW process is negligible, causing insufficient plastic flow in the bottom of the workpiece, which leads to the formation of tunneling defect in the area. The formation of such defects will severely deteriorate the quality of the final joint (Mubiayi et al., 2018). According to the results presented in Figs. 10 and 11, the significant change of YS and UTS parameters can be observed in each of the three processes by changing the cone angle. As it is obvious, by increasing the cone angle, YS and UTS of the SFWS welded specimens were increased with considerable slopes. Regarding the diagrams for SFSW process, it can be concluded that the use of the tool with 15° cone angle provided the optimum mechanical properties of the joint. In this case, YS and UTS experienced the respective increases of 40% and 17% compared to the base case (cylindrical pin). Based on the obtained results, further increase of the cone angle from 15° in SFSW would result in a decrease in YS and UTS, which can be attributed to the decrease in the plastic flow at the bottom of the workpiece. As it is apparent, by increasing the cone angle, the volume of the generated horizontal flow decreased as a result of reduction in the pin diameter. This would lead to the loss of mechanical quality of joint.

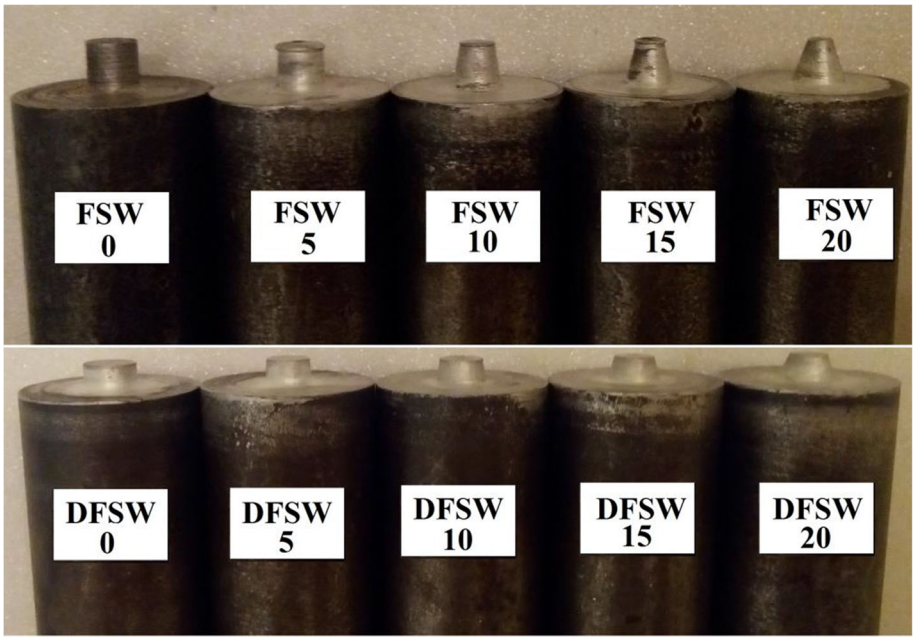

Fig. 3 The used tools in the FSW and DFSW processes

According to the presented diagrams in Figs. 10 and 11, it was found that in both symmetric and asymmetric DFSW processes, the mechanical properties of the joint at the most of the cone angles were higher than the SFSW process with the same angle. This is due to the improved mechanical bonding properties in DFSW processes.

In the DFSW process, since both sides were welded, the material flow was formed properly in the upper and lower surfaces of the specimen. The presence of the sufficient material flow resulted in eliminating the formation possibility of tunneling and cavity imperfections. Elimination of these imperfections enhanced the process quality, and consequently, the mechanical properties of the final joint were increased significantly. The results highlighted that the optimum pin angle was 10° in both DFSW processes, which was associated with the highest mechanical properties. The increments of YS and UTS for the symmetric DFSW process (10° angle) compared to the peak state of the SFSW process (15° angle) were equal to 5.4% and 3.7%, respectively. These increments for asymmetric DFSW process were the respective values of 13.5% and 22.7%. The results implied the superior mechanical properties of asymmetric DFSW specimens compared to symmetric DFSW in all studied cone angles. According to the former studies, the mechanical and microhardness properties of RS region were generally more favorable than AS region (Mishra et al., 2014), which can be attributed to the considerable and sufficient plastic flow in RS region. The presence of relatively smaller material flows in AS region reduced the microstructure modification besides the concentration of defects, and consequently, a decrease in the mechanical properties of the final joint was achieved. The quality of the joint and mechanical properties can be significantly improved by strengthening the AS region of the welded specimen.

By applying the asymmetric technique in DFSW process, half of the workpiece thickness on either side of the weld line will be placed in the AS region and the other half would be in the RS region. This strengthens the upper

Table 3 Design of experiments (DOE)

Model's name	Process	Tapered angle (°)
A0	FSW	0
A5		5
A10		10
A15		15
A20		20
B0	Symmetrical DFSW	0
B5		5
B10		10
B15		15
B20		20
C0	Asymmetrical DFSW	0
C5		5
C10		10
C15		15
C20		20

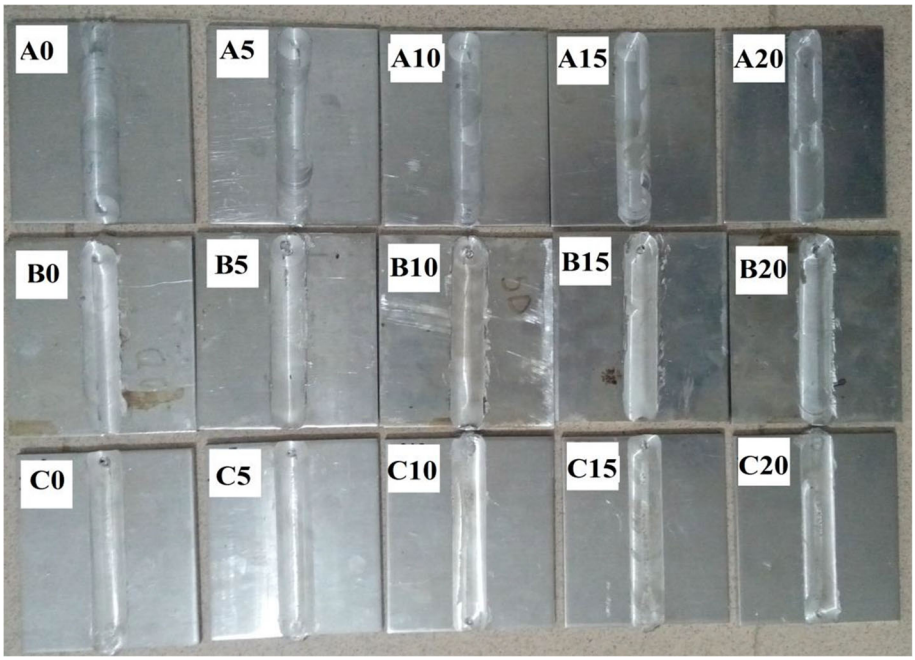

Fig. 4 The welded specimens

and lower AS regions of the welded specimen that is followed by the reduction in the defect concentration on both sides of the weld. Therefore, the better mechanical quality of the joint will be seen at all cone angles in the asymmetric DFSW than the symmetric DFSW. According to the obtained results, the final fracture location in the SFSW process was generally in the AS region. However, the fracture location was changed through the use of asymmetric DFSW. As mentioned, in asymmetric DFSW process, regarding the mixing of AS and RS regions in the weld section, a symmetric flow was created at both sides of the weld line across the thickness. Hence, in accordance with Table 4, it can be understood that in all asymmetric DFSW specimens, the final fracture occurred in NZ region. Fracture occurrence in the middle region of the welded specimen indicated the approximately similar plastic flow concentration on both sides of the weld line, which minimized the possibility of defect formation. The specimens before and after the tensile test as well as their fracture location are depicted in Fig. 12.

Based on the presented results, it was found that the use of DFSW process would result in a significant increase in the mechanical quality of the joint in comparison with SFSW. The YS, UTS, and E% of the peak

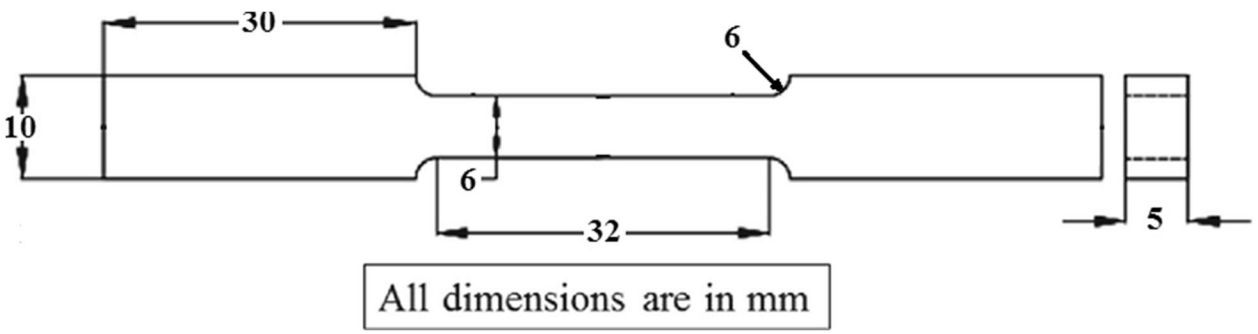

Fig. 5 Schematic of the tensile test specimen

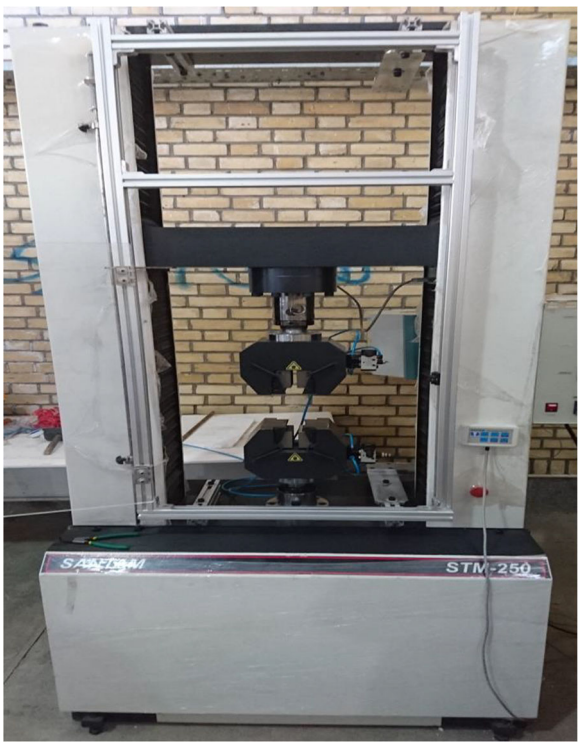

Fig. 6 The used tensile testing machine

samples of three welding processes were compared with respect to the mechanical properties of the base metal in Fig. 13.

According to Fig. 13, it was found that the peak sample of asymmetric DFSW gained the closest mechanical properties to the base metal. The YS, UTS, and E% parameters in this sample were 78.3%, 84.8%, and 86.4% of the base metal, respectively. It means that the mechanical properties of the final joint obtained by this welding method were mostly similar to the properties of the base material.

Hardness test

In this section, the hardness patterns of the welded specimens and their distributions along the weld section are investigated. The Vickers hardness of SFSW and symmetric and asymmetric DFSW welded specimens with different cone angles are presented in Figs. 14, 15, and 16, respectively.

According to the diagrams presented in Figs. 14, 15, and 16, regardless of the performed welding process, the hardness distribution pattern in the weld sections of all samples was a W-shaped pattern, which was consistent with the pattern obtained by most of the conducted researches in this area [20]. In all samples, the hardness of NZ, TMAZ, and HAZ regions were significantly lower than the hardness of the base metal due to the thermal softening of these areas owing to the relatively large thermal cycles. By moving away from the welding center and approaching the outer boundaries of HAZ region, the hardness of the sample reached the hardness of the base metal (in the range of 95–105). Regardless of the welding process, the lowest hardness values (in the range of 50–65) and highest hardness reductions occurred in the HAZ region in all specimens considering the thermal softening and lack of plastic flow. After HAZ zone, the lowest values of hardness corresponded to TMAZ and NZ regions.

Since NZ region endured large plastic material flow besides the change in grain size, higher hardness values were recorded in this section compared to other weld sections. In

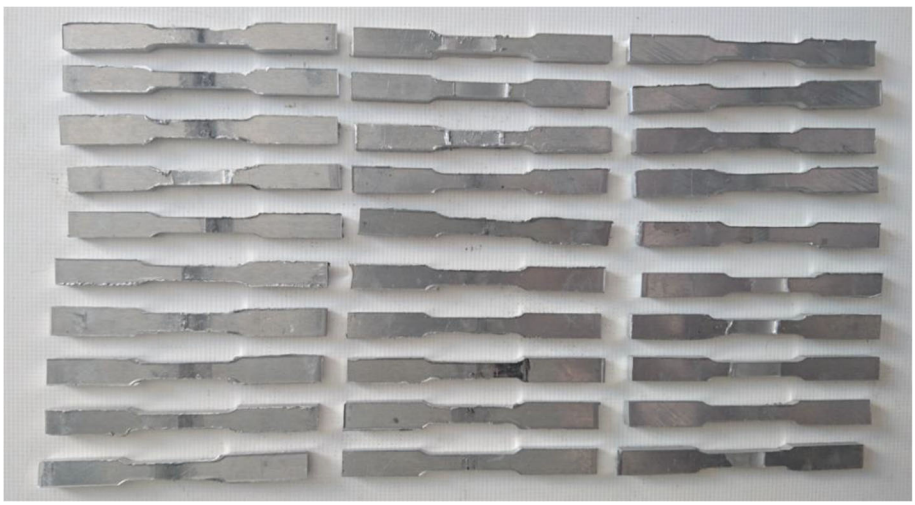

Fig. 7 The cut view of the tensile test specimens

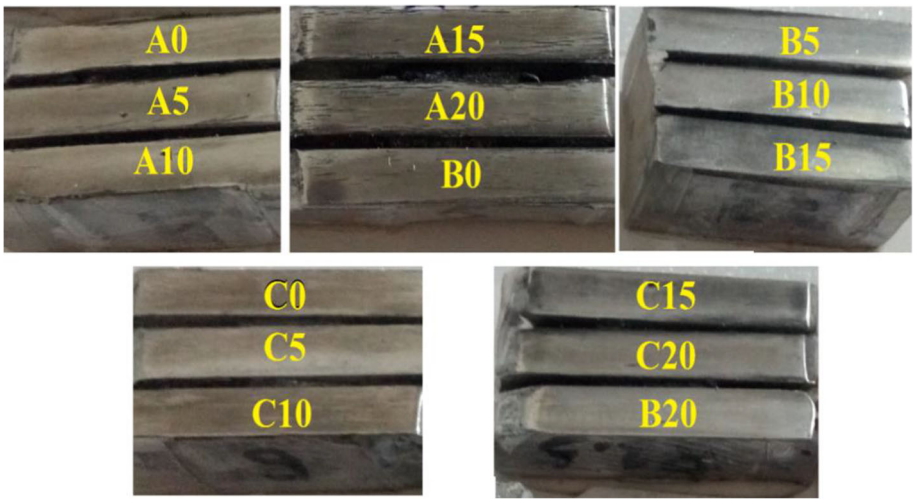

Fig. 8 The prepared samples for microhardness testing

the NZ region, due to the large plastic material flow and high thermal energy close to the melting temperature, dynamic recrystallization occurred, which was followed by the microstructural modification. Due to the inverse relation of hardness and grain size (Mubiayi et al., 2018), decreasing the grain size in the NZ region resulted in an increase in the hardness compared to other weld sections. According to Figs. 14 and 15, it was found that in SFSW and symmetric DFSW processes, the lowest hardness occurred in HAZ of AS region. This correlated to the asymmetric heat

Fig. 9 The used equipment for microhardness testing

Table 4 Tensile test results of the studied specimens

Process	Sample	YS (Mpa)	UTS (Mpa)	%E	Fracture location
	Base	**268**	**311**	**17**	**Middle**
SFSW	A0	132	179	8.3	AS-HAZ
	A5	146	181	9.1	NZ
	A10	163	201	10.5	NZ
	A15	185	215	12.2	AS-TMAZ
	A20	174	210	11.8	AS-HAZ
Symmetrical DFSW	B0	148	192	10.4	AS-TMAZ
	B5	176	207	12.1	AS-TMAZ
	B10	195	223	12.9	AS-TMAZ
	B15	186	214	13.2	AS-TMAZ
	B20	165	196	12.4	NZ
Asymmetrical DFSW	C0	181	231	11.6	NZ
	C5	192	249	13.9	NZ
	C10	210	264	14.7	NZ
	C15	201	243	14.2	NZ
	C20	185	214	13.3	NZ

distribution and uniform plastic flow in this region compared to the RS region. Generally, in all cases with different cone angles in SFSW and symmetric DFSW processes, the hardness in AS region was lower than RS region. This was confirmed by the conducted tensile tests regarding the fracture occurrence in these areas.

In asymmetric DFSW welded specimens, due to the overlapping of AS and RS regions in sides of the weld line as well as the relatively symmetric plastic flows, the symmetric W-shaped patterns were formed on both sides of the weld sections. According to Fig. 16, by increasing the cone angle of the tool to 10°, due to the increase in the plastic flow of the material, more microstructural modifications were performed in the NZ region as a result of increase in the material plastic flow. Therefore, the hardness of the specimen was increased in the NZ.

Conclusion

The effect of cone angle on the mechanical and microhardness properties of specimens obtained from SFSW, symmetric DFSW, and asymmetric DFSW jointing of AA6061-T6 alloy was investigated in this paper. In the mentioned welding processes, 5 tools with 5 different cone angles of 0, 5, 10, 15, and 20° were used, and their effects on the mechanical properties of the welded

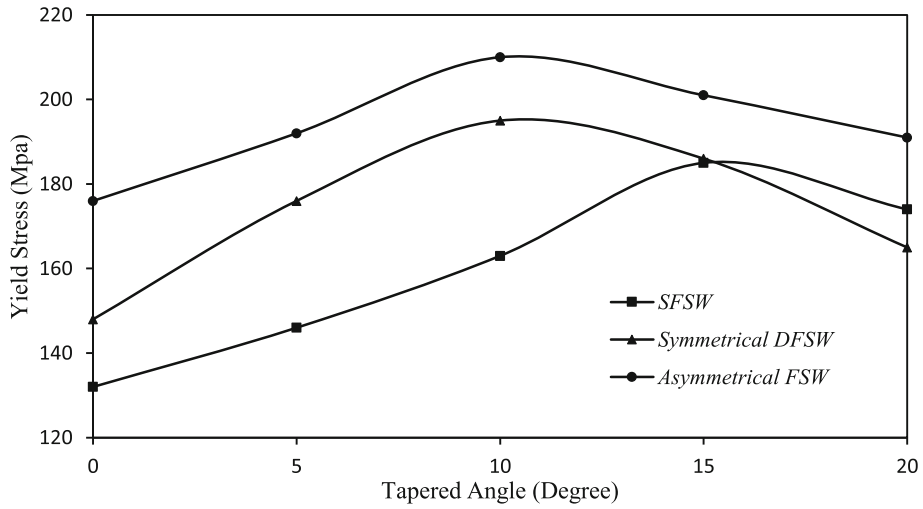

Fig. 10 Comparison of YS for three mentioned processes at different cone angles

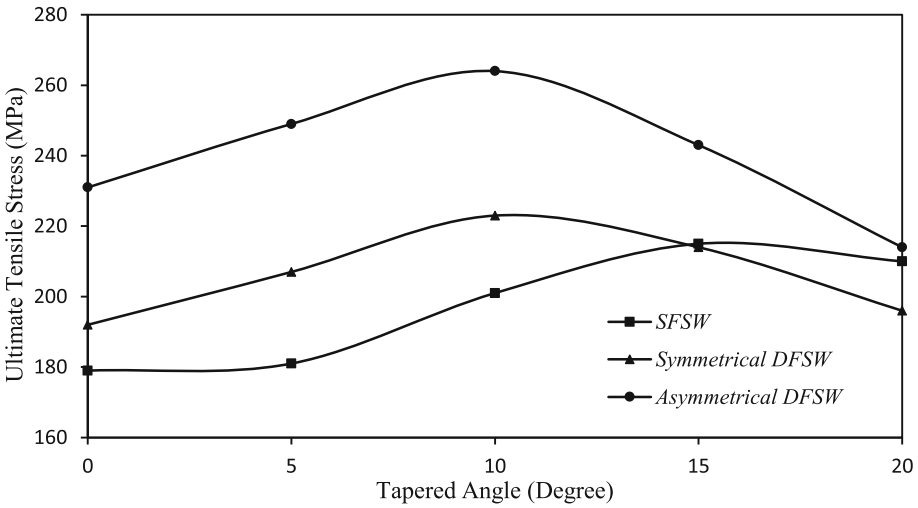

Fig. 11 Comparison of UTS for three mentioned processes at different cone angles

specimens were examined. The most important results of this paper can be summarized as follows:

- It was found that in all of the three mentioned processes, changing the cone angle of the tool resulted in the changes of YS, UTS, and E% parameters.
- The final fracture location of the welded specimen in the tensile test was significantly dependent on the process type. In SFSW and symmetric DFSW processes, specimen fracture generally occurred in the AS region, while in DFSW asymmetric the fracture occurred in NZ region.
- In general, all welded specimens with conical pins exhibited superior mechanical properties compared to cylindrical pins.
- Both symmetric and asymmetric DFSW processes experienced significant growth at most of the cone

Fig. 12 The fracture location of the studied samples

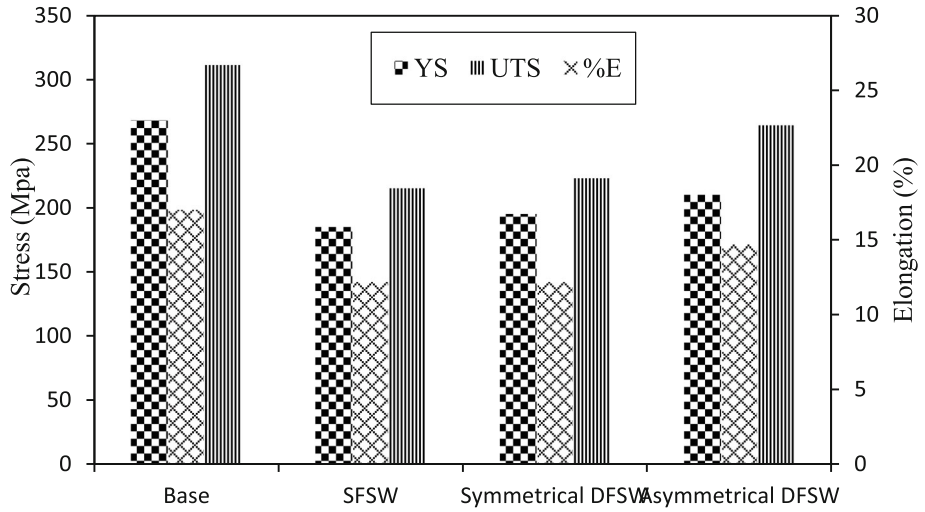

Fig. 13 The comparison of the mechanical properties for three welding process with base metal properties

angles relative to the SFSW process. This indicated the superiority of DFSW processes over SFSW.

- The peak angle was 10° in conical pins from the improved mechanical properties points of view in both symmetric and asymmetric DFSW processes.
- In the SFSW process, using a 15° cone angle resulted in the highest mechanical properties. In this case, YS, UTS, and E% experienced 40%, 17%, and 46.9% growth, respectively compared to the base case (cylindrical pin).
- The increase of YS, UTS, and E% for the symmetric DFSW process (10° angle) compared to the SFSW process peak state (15° angle) was 5.4%, 3.7%, and 5.7%, respectively. For the asymmetric DFSW peak state (10° angle) compared to the SFSW peak state (15° angle), the increase in the mentioned values was corresponding to 13.5%, 22.7%, and 20%.
- The asymmetric DFSW peak samples had the closest mechanical properties to the base metal, in which YS, UTS, and E% parameters were 78.3%, 84.8%, and 86.4% of the base metal, respectively.
- Regardless of the type of welding process, the lowest hardness values in all samples occurred in the HAZ region. After HAZ region, the TMAZ and NZ regions attained the lowest hardness compared to the base material.

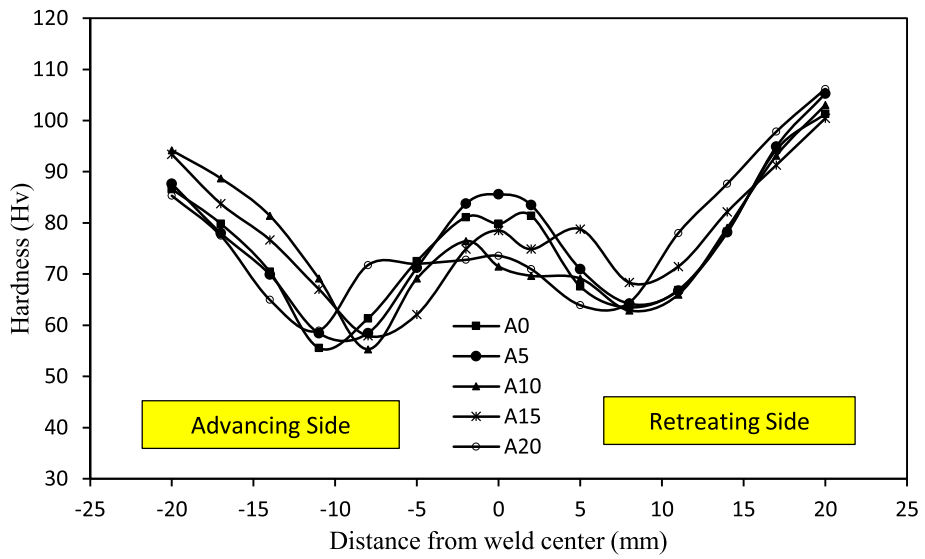

Fig. 14 Microhardness distribution of SFSW samples at different cone angles

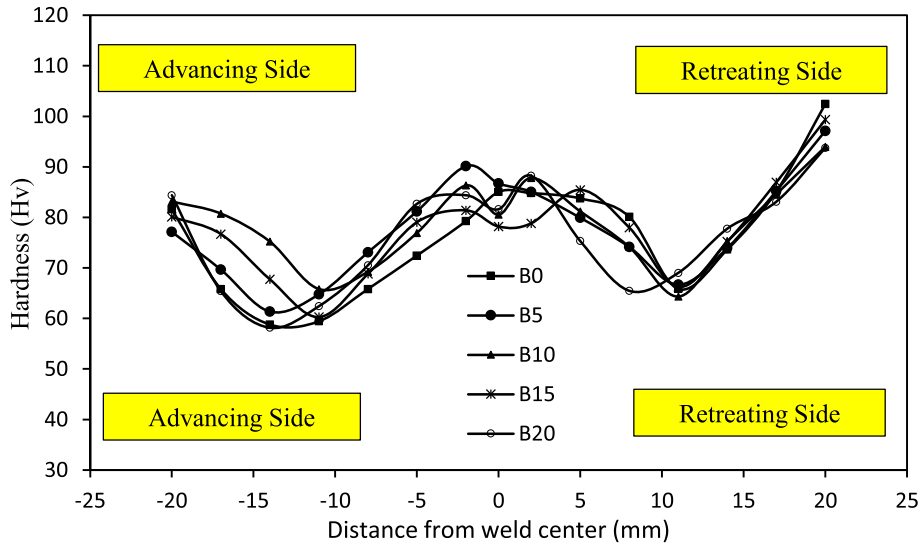

Fig. 15 Microhardness distribution of symmetric DFSW samples at different cone angles

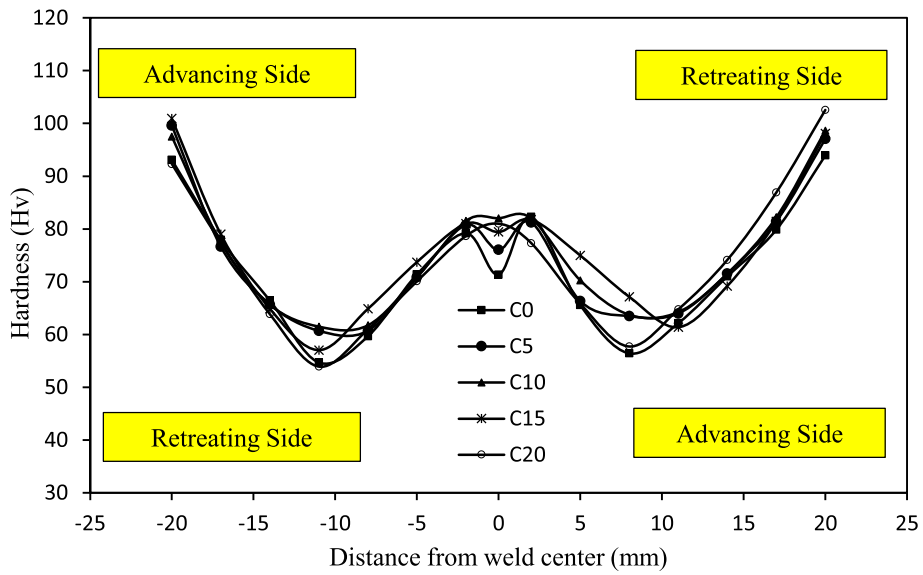

Fig. 16 Microhardness distribution of asymmetric DFSW samples at different cone angles

- In general, for all cases with different cone angles in SFSW and symmetric DFSW processes, hardness values in the AS region were lower than RS region. Tensile tests also confirmed this justification regarding the fracture occurrence in these areas.
- In the asymmetric DFSW-welded specimens, due to the overlapping of AS and RS regions in two sides of the weld line at two welding passes, relatively symmetric thermal cycles and plastic flow were formed at the weld section, which resulted in the formation of a symmetric W-shaped microstructure at the welded cross-section.

Abbreviations

FSW: Friction stir welding; UTS: Ultimate tensile strength; CCD: Central composite design

Acknowledgements

The authors gratefully acknowledge the financial support by the Malayer University of Iran under Grant No. 84/9-1-462.

Authors' contributions

The authors read and corrected the manuscript. The authors read and approved the final manuscript.

Funding

The financial support by the Malayer University of Iran under Grant No. 84/9-1-462.

Availability of data and materials

All data analyzed during this study are available from the corresponding author on request.

Declarations

Competing interests

The authors declare that they have no competing interests.

Author details

[1]Department of Mechanical Engineering, Faculty of Engineering, Malayer University, Malayer, Iran. [2]Department of Mechanical Engineering, Tabriz University, Tabriz, Iran.

Received: 25 May 2020 Accepted: 3 June 2021
Published online: 12 June 2021

References

Astm, E. (1997). 8: Standard test method for tensile testing of metallic materials. In *Annual book of ASTM standards, vol. 3*.

Baker, T., Rahimi, S., Wei, B., He, K., & McPherson, N. (2019). Evolution of microstructure during double-sided friction stir welding of microalloyed steel. *Metallurgical and Materials Transactions A*, *50*(6), 2748–2764. https://doi.org/10.1007/s11661-019-05184-2.

Devaiah, D., Kishore, K., & Laxminarayana, P. (2018). Optimal FSW process parameters for dissimilar aluminium alloys (AA5083 and AA6061) using Taguchi technique. *Materials Today: Proceedings*, *5*(2), 4607–4614.

Dialami, N., Cervera, M., Chiumenti, M., & de Saracibar, C. A. (2017). Local–global strategy for the prediction of residual stresses in FSW processes. *The International Journal of Advanced Manufacturing Technology*, *88*(9-12), 3099–3111. https://doi.org/10.1007/s00170-016-9016-3.

Gadakh, V. S., & Adepu, K. (2013). Heat generation model for taper cylindrical pin profile in FSW. *Journal of Materials Research and Technology*, *2*(4), 370–375. https://doi.org/10.1016/j.jmrt.2013.10.003.

Ghiasvand, A., Kazemi, M., Mahdipour Jalilian, M., Ahmadi Rashid, H. (2020). Effects of tool offset, pin offset, and alloys position on maximum temperature in dissimilar FSW of AA6061 and AA5086. International Journal of Mechanical and Materials Engineering 15 (1)

Ghiasvand, A., Kazemi, M., Mahdipour Jalilian, M. (2021). Numerical investigation and prediction of grain Size in different welding areas of AA6061 Aluminum alloy. Amirkabir Journal of Mechanical Engineering 53 (6), 20-20

Hejazi, I., & Mirsalehi, S. E. (2016). Effect of pin penetration depth on double-sided friction stir welded joints of AA6061-T913 alloy. *Transactions of Nonferrous Metals Society of China*, *26*(3), 676–683. https://doi.org/10.1016/S1003-6326(16)64158-4.

Kumar, A. R., Varghese, S., & Sivapragash, M. (2012). A comparative study of the mechanical properties of single and double sided friction stir welded aluminium joints. *Procedia Engineering*, *38*, 3951–3961. https://doi.org/10.1016/j.proeng.2012.06.452.

Lohwasser, D., & Chen, Z. (2009). *Friction stir welding: From basics to applications*. Elsevier.

Mishra, R. S., De, P. S., & Kumar, N. (2014). *Friction stir welding and processing: Science and engineering*. Springer. https://doi.org/10.1007/978-3-319-07043-8.

Mubiayi, M. P., Akinlabi, E. T., & Makhatha, M. E. (2018). *Current trends in friction stir welding (FSW) and friction stir spot welding (FSSW): An overview and case studies*. Springer.

Rai, R., De, A., Bhadeshia, H., & DebRoy, T. (2011). Friction stir welding tools. *Science and Technology of Welding and Joining*, *16*(4), 325–342. https://doi.org/10.1179/1362171811Y.0000000023.

Ramachandran, K., Murugan, N., & Kumar, S. S. (2015). Effect of tool axis offset and geometry of tool pin profile on the characteristics of friction stir welded dissimilar joints of aluminum alloy AA5052 and HSLA steel. *Materials Science And Engineering: A*, *639*, 219–233. https://doi.org/10.1016/j.msea.2015.04.089.

Totten, G. E. (2006). *Steel heat treatment handbook, -2 volume set*. CRC press. https://doi.org/10.1201/9781482293029.

Ugender, S., Kumar, A., & Reddy, A. S. (2014). Experimental investigation of tool geometry on mechanical properties of friction stir welding of AA 2014 aluminium alloy. *Procedia Materials Science*, *5*, 824–831. https://doi.org/10.1016/j.mspro.2014.07.334.

Xu, W., Wang, H., Luo, Y., Li, W., & Fu, M. (2018). Mechanical behavior of 7085-T7452 aluminum alloy thick plate joint produced by double-sided friction stir welding: Effect of welding parameters and strain rates. *Journal of Manufacturing Processes*, *35*, 261–270. https://doi.org/10.1016/j.jmapro.2018.07.028.

Yaduwanshi, D., Bag, S., & Pal, S. (2018). On the effect of tool offset in hybrid-FSW of copper-aluminium alloy. *Materials and Manufacturing Processes*, *33*(3), 277–287. https://doi.org/10.1080/10426914.2017.1279309.

Yang, J., Wang, D., Xiao, B., Ni, D., & Ma, Z. (2013). Effects of rotation rates on microstructure, mechanical properties, and fracture behavior of friction stir-welded (FSW) AZ31 magnesium alloy. *Metallurgical and Materials Transactions A*, *44*(1), 517–530. https://doi.org/10.1007/s11661-012-1373-4.

Zettler, R., Lomolino, S., dos Santos, J. F., Donath, T., Beckmann, F., Lippman, T., & Lohwasser, D. (2005). Effect of tool geometry and process parameters on material flow in FSW of an AA 2024-T351 alloy. *Welding in the World*, *49*(3-4), 41–46. https://doi.org/10.1007/BF03266474.

Zhang, Y., Cao, X., Larose, S., & Wanjara, P. (2012). Review of tools for friction stir welding and processing. *Canadian Metallurgical Quarterly*, *51*(3), 250–261. https://doi.org/10.1179/1879139512Y.0000000015.

Publisher's Note